www.sciencemag.org/content/349/6243/78/suppl/DC1

Supplementary Materials for

Shape-selective zeolite catalysis for bioplastics production

Michiel Dusselier,* Pieter Van Wouwe, Annelies Dewaele, Pierre A. Jacobs, Bert F. Sels*

*Corresponding author. E-mail: michiel.dusselier@gmail.com (M.D.); bert.sels@biw.kuleuven.be (B.F.S.)

Published 3 July 2015, *Science* **349**, 78 (2015)
DOI: 10.1126/science.aaa7169

This PDF file includes:

Materials and Methods

Materials

Commercial acidic H-Beta catalysts were received or purchased from Süd-Chemie AG (now Clariant). H-USY (of the CBV series) and NH_4-Beta zeolites were purchased from Zeolyst (PQ). Used commercial zeolites: H-Beta with bulk Si/Al 12.5, 75 and 180 (Süd-Chemie) and H-USY CBV600 with bulk Si/Al 2.6. The framework Si/Al of USY CBV600 is 9.5, with 27% of framework Al (as determined by Al-NMR) (*30*), resulting from steaming of this commercial material during its preparation. The framework ratios are used to calculate the amount of Brønsted acid sites of the zeolites. NH_4-Beta Si/Al 12.5 purchased from Zeolyst (CP814E) and used in its H-form after calcination, was showing identical results as the Süd-Chemie H-Beta Si/Al 12.5 catalyst.

NAFION NR50, p-toluenesulfonic acid, sulfuric acid (97%), Amberlyst® 15 wet hydrogen form and H-Al-MCM-41 catalyst (CAS 1318-02-1, 2.5-3 nm pore diameter, 3% Al) were purchased from Sigma-Aldrich. L,L and D,D-lactide was donated by Purac (now Corbion Purac). 50 and 90 wt% aqueous solutions of L-Lactic acid (L-LA) were purchased from Sigma-Aldrich and used as received. Solutions of 20 wt% were made by dilution followed by equilibration at 70°C for 1 week to let the solutions converge to their equilibrium monomer-oligomer composition, as verified by HPLC and ^{1}H-NMR and in line with literature (*14, 31, 32*). HPLC grade reaction solvents (aromatics) and analysis solvents (acetonitrile, DMSO-d6, $CDCl_3$) were obtained from Acros Organics, Fisher Scientific or Sigma-Aldrich and used as received. (R)-α-hydroxybutryic acid was obtained from Sigma-Aldrich. Racemic-α-hydroxybutenoic acid (a.k.a. methyl vinylglycolate) was obtained from TCI-Europe and fully hydrolyzed (as confirmed by ^{1}H-NMR) with acidic resin Amberlyst-15 prior to use as substrate. Materials used in the synthesis of the custom H-Beta zeolite were tetraethylorthosilicate (Acros), tetraethyl-ammonium hydroxide (40 wt%, Aldrich), HF (Chemlab), and metallic Al (UCB).

Methods

Catalyst treatments

Zeolite catalysts were calcined prior to use for 6 h at 823 K, reached at a rate of 1 K per minute under static air. Regeneration of catalysts in the re-use study was performed identically.

Reaction procedures

In a typical reaction, to 0.5 g of air-equilibrated H-Beta (corresponding to 0.45 g of dry zeolite, as it contains 10 % of water according to thermogravimetric analysis; Si/Al 12.5) in a 25 mL round bottom flask, the desired amount of L-LA was added. Usually the latter amounted to 1.67 g of 50 wt% LA in water, sometimes to 1 g of a 90 wt% LA in water solution. Then 10 mL of solvent was added (*e.g.* toluene or o-xylene) as well as a magnetic stirring bar. On top of the round bottom flask, a custom made phase-settler / solvent reflux trap was installed, filled beforehand with the same reaction solvent as in the flask (approximate volume of 16 mL). On top of the phase-settler, a condenser was put in place via ground joints. This setup assures reflux of the lighter solvent phase and trapping of the water. The solvent floats on top and moves to the flask through the glass-tube in the middle while the water sinks to the bottom of the trap where it accumulates.

At the start of the reaction, the flask is submerged in a pre-heated stirred temperature-controlled oil bath. The bath is typically held at 413 (or 403) K for toluene reactions and 443 K for o-xylene reactions, slightly exceeding the boiling point of the respective solvents to assure reflux. Under continuous stirring of the mixture under solvent reflux and water-removal conditions, the reaction is carried out for times varying between 0.25 and 3 h under constant solvent and reaction volume (with exception of the initial fast removal of the excess water of the aqueous solution; *e.g.* 100 mg in case of 1 g of 90 wt% LA feed). For determination of kinetics and time-profiles, identical reactions were run in parallel and stopped at different time intervals. This is needed to avoid experimental analytical errors found when taking intermediate samples during reaction due to the complexity of the setup and refluxing phase. For work under reduced pressure and thus different reaction temperatures (for apparent activation energy determination), a vacuum line with adjustable pressure output was attached on top of the condenser. The reduced pressure reflux temperature was measured during reaction. On-line temperature (-time) profiles were also recorded during test-reactions in toluene (at 3 different pressures) and o-xylene. A scheme of the general lab-scale reaction setup is shown in Fig. S1.

Reaction analysis

Analyzing mixtures of lactide, lactic acid and oligomers in presence of an organic solvent is not straightforward. High pressure liquid chromatography (HPLC), gas chromatography (GC) and proton nuclear magnetic resonance spectroscopy (^{1}H-NMR) were adapted for this analysis and compared. Possible analytic pitfalls are disclosed below. The work-up procedure of the reaction mixture is also crucial to an accurate analysis.

Work-up

After reaction, the batch reactor contains the (solid) catalysts, the reflux solvent, lactide, lactic acid and linear oligomers of lactic acid. As not all of the organic species (partially or completely) dissolve in the solvent at room temperature (*e.g.* lactic acid in toluene), the mixture was homogenized by addition of 12 mL of acetonitrile. This addition turns the liquid phase into a clear and homogeneous one. Indeed, acetonitrile is known to dissolve all possible kinds of lactyl species (*14, 31*) (acetonitrile is also to some extent a solvent for PLLA polymers). After homogenization, removal of zeolite (or other solid catalysts) by filtration over a glass frit filter with the aid of a vacuum pump is facilitated. After the first filtration, the solids on the filter are mixed with another 6 mL of acetonitrile allowing extraction of sorbed organic species, before another filtration. The total volume of the filtered homogeneous reaction solution determined in a graduated cylinder, usually amounts to 25-30 mL. On this solution, three independent analytical methods for determining product yields and LA conversion were performed (^{1}H-NMR, HPLC and chiral GC). The yield of lactide can be measured by all three techniques. The conversion of lactic acid and the yields of lactyl oligomers (L_nA, $n \geq 2$) can be measured accurately only by HPLC and NMR. Due to the limited volatility of (oligo)lactic acid and the occurrence of thermal reactions with lactyl oligomers in the inlet port, the use of GC is excluded for their quantification.

^{1}H-NMR

From the homogeneous worked-up reaction mixture two 1 mL samples were taken and dried in a mildly flowing N_2-atmosphere to remove toluene and acetonitrile solvents. Gentle drying in N_2-atmosphere allows solvent removal, not affecting the less volatile organic reaction species. This was verified by subjecting known lactide and lactic acid mixtures to this treatment. One dry sample is dissolved in 0.7 mL of $CDCl_3$ and the other in 0.7 mL of DMSO-d_6. Both samples were shaken till homogeneous, transferred to NMR tubes and measured on a Bruker Avance-300 MHz NMR-spectrometer with automated sampler. Analyzing the distribution of lactic acid species is done in the methyl (1 to 1.8 ppm) or methine region (4 to 5.8 ppm), since all species obtained by condensation chemistry share the presence of CH-CH_3 units in their structure. This method is largely based on the analytical work by Espartero *et al* (*32*). Analysis performed on DMSO-d_6 samples in the methine region allows distinguishing between meso-lactide, L,L-lactide (same shifts as D,D-lactide), the center lactyl units of linear oligomers, the –COOH and –OH end groups of linear oligomers as well as monomeric lactic acid. The $CDCl_3$ sample is used as backup for the lactide determination with respect to the other lactyl species present. This is especially useful for low conversion samples, where acidic protons from LA could interfere with the analysis in DMSO-d_6 as they show broad NMR signals in the lactide region. In these cases, $CDCl_3$ solvent samples can be used for accurate lactide determination. Due to overlapping shifts of the methine quartets of other lactyl species in $CDCl_3$, this solvent does not allow to determine accurate lactic acid and oligomer distributions.

A typical ^{1}H-NMR sample series in DMSO-d_6 in the methine region is shown in Fig. S2A. It shows the transformation of lactic acid into lactide in time of three reaction mixtures stopped at different times compared to the spectrum of the 90 wt% aqueous LA feedstock. This feed typically contains around 35 % of oligomers at the start (25 % L_2A). Initial presence of oligomers in this feedstock is very clear from the first spectrum (*14, 31, 32*) and will be discussed in detail below (*14*). Typically, the productyield, LA conversion and oligomeric side-product formation were determined by ^{1}H-NMR integration, relative to the total amount of lactyl-containing products present. The number average length of the oligomer fraction can easily be determined via end-group analysis (Espartero *et al.* (*32*)) because of the clear difference in chemical shift between center lactyl units and both end group lactyls (Fig. S2). The product yields and LA conversion and thus the distribution of all condensation species can accurately be determined as such, since no other products but condensation products were found in the reaction mixtures (as confirmed by HPLC, GC and GC-MS). Further verification of the ^{1}H-NMR obtained lactide yields was performed by comparing yields obtained by GC and HPLC (analysis methodology, see below). The lactide yields from these three techniques were in good agreement with one another (< 5% difference), provided that analytical care was taken in GC (inlet port temperature) and HPLC analyses, as explained below. The best results in the paper, high lactide yields of Fig. 2B and 3 have been performed at least in triplicate with variations less than 3%.

As an example, the ^{1}H-NMR methyl region of two different feedstocks is shown in Fig. S2B. The analyses of the feedstocks in the ^{1}H-NMR methine region was in agreement with the oligomer distribution measured with HPLC (Fig. S3) and in line with the standard results by Vu *et al.* (*14*).

Gas chromatography (GC)

GC analysis was performed on a Hewlet Packard 6890 with a chiral 25 m Agilent WCOT fused silica CP-Chirasil-DEX CB capillary column with internal diameter of 0.32 mm and film thickness of 0.25 μm, equipped with an FID detector held at 548 K, and ChemStation software. The injection port temperature was 498 K and the initial column temperature was set at 343 K. This temperature is held for 5 minutes before being ramped to 423 K at 15 $K.min^{-1}$. After 5 minutes at 423 K, the oven is ramped to 523 K at 25 $K.min^{-1}$ and held there for 5 minutes. This chiral GC methodology allows to separate L,L-lactide, D,D-lactide and meso-lactide (D,L-diastereo-isomer). Quantification of lactides in the toluene/acetonitrile solvent mixtures obtained from the work-up was performed with calibration curves using naphthalene as external standard and the total volume of the worked-up reaction mixture. Whereas GC analysis of reaction mixtures relatively rich in lactides is accurate, two problems can offset this accuracy: i) the presence of high amounts of oligomers of lactic acid; they tend to react in the in the GC injection port and produce lactides by thermal backbiting, rendering it hard to quantify the inherent lactide produced by the catalytic reaction; and ii) the high temperature of the injection port; it can give rise to racemization of lactides, as evidenced by meso-lactide detection upon injecting solutions of pure L,L-lactide standards (at too high inlet temperatures). GC analysis at appropriate inlet temperatures (up to 498 K) is therefore suited to analyze mixtures rich in lactide, but not intermediate or low in lactide, since the latter are rich in oligomers of lactic acid. Lactic acid itself cannot be accurately quantified by GC due to its limited volatility. Generally, GC was only used as secondary confirmation tool confirming high yields of lactide produced by optimized catalytic reactions and assessing the degree of meso-lactide formation by racemization. The absence of other organic species in GC(-MS), possibly derived from side reactions of lactic acid during the reaction, confirmed the selectivity of the reaction towards condensation products and corroborated the ^{1}H-NMR analysis. Additional GC analysis of the reflux solvent reservoir in the phase separator (P1 in Fig. 3) never allowed detection of trace amounts of lactide, the most volatile of all formed lactyl compounds. This confirmed that no organic species were transferred to the trap by the reflux conditions.

High Pressure Liquid Chromatography (HPLC)

After exact determination of the total volume of the worked-up reaction mixture, a 1 mL sample was taken and dried under flowing N_2-atmosphere to remove toluene and acetonitrile solvents. The dry sample was dissolved in 1 mL of a 50:50 V:V water:acetonitrile mixture and analyzed with Reverse Phase-HPLC on a Thermo Separation P4000 Products Spectra System equipped with prevail C_{18} column and an SPD10 UV-Vis detector at 210 nm. Two solvents are used in the elution program: a) water/acetonitrile 95/5 (V/V, with addition of 2 mL of 85% H_3PO_4 per L); b) 100% acetonitrile (with addition of 2 mL of 85% H_3PO_4 per L). The elution program (a/b, V/V) was as follows: minute 0-1: 100/0; minute 1-15: linear ramp to 20/80; minute 15-20: 20/80; and minute 18-30: return to 100/0. The water:acetonitrile phase both as sample solvent and in the eluent program assures full dissolution and separation of LA and the short hydrophilic lactic acid oligomers (L_nA, with $n < 5$), as well as lactide and the more apolar longer oligomers (L_nA with $n \geq 5$). Both eluents are acidified to assure protonation of all acidic species, allowing their separation as neutral compounds. This method is

largely based on the analytical work by Vu *et al.* on the distribution of oligomers in concentrated lactic acid solutions (*14*). The determination of lactide yields via HPLC was performed with a linear calibration of known concentrations.

HPLC analysis is reliable and allows determination of LA conversion and yields of all lactyl species involved. In contrast to ^{1}H-NMR, which provides a number average oligomer length, HPLC analysis can separate all oligomers encountered. The number average oligomer length based on HPLC profiles and the ones from ^{1}H-NMR were always in good agreement (*e.g.* Fig S5A). The major pitfall with this analysis method is the time between dissolution of the dried sample and the actual injection. It was found that the oligomeric species and especially lactide are prone to hydrolysis due to excess water in the sample solvent. If a lactide standard dissolved in water:acetonitrile is left standing for 4 h, L_2A can already be detected (in progressive amounts with time) due to hydrolysis. This renders NMR more suited for large numbers of samples.

As an example, HPLC analysis of two L-LA aqueous feedstock solutions is shown in Fig. S3. Their composition is in line with ^{1}H-NMR analysis and literature (*14*) and based on the equilibria associated with LA oligomerization. Lactide is always absent in the feedstock.

Productivity calculations

Volumetric productivities were calculated from lactide yields (^{1}H-NMR), the input lactic acid weight and the volume of organic solvent in the reactor (usually 10 mL). A lactide yield of 50% was reached using 3.34 g of a 50 wt% L-LA solution (initially present and fastly removed water volume not included in calculation) with 1g of (air-equilibrated) H-Beta (Si/Al 12.5) after 15 minutes of reaction in 10 mL of o-xylene with the oil bath at 443 K. This translates to 267 g of lactide per L reaction solvent per hour. Per gram of dry zeolite catalyst, this translates into 3.0 $g_{lactide}/g_{zeolite}.h^{-1}$.

Catalyst characterization

Scanning electron microscopy (SEM) was performed on a Philips XL FEG30 (Fig S6) and on a JEOL JSM-6010 JV microscope (Fig S12), to assess the morphologies of the zeolites. The energy of the Betam was varied between 5 and 30 kV, visualizing several magnification levels. Secondary and back-scattered electrons are used to make images of the surface. Samples were coated with gold prior to measurement using a JEOL JSC-1300 sputter.

Inductively coupled plasma/atomic emission spectroscopy (ICP/AES) allowed elemental analyses of the Si and Al content of the zeolites. It was performed on a Perkin Elmer Optima DV 3300 ICP-AES at 396.2 nm, after dissolving the solid zeolite samples. The Si/Al ratio of the zeolites was in good agreement with the values provided by the supplier, *i.e.* H-Beta with Si/Al of 12.5 (from the supplier) was found to have a Si/Al ratio of 12.9.

Powder X-ray diffraction (PXRD) were recorded on powder samples on a STOE Stadi P diffractometer equipped with Cu-$K_{\alpha 1}$ source and IP-PSD detector.

Thermogravimetric analysis (TGA) allowed determining the moisture content of air-equilibrated zeolites. It was performed under nitrogen using a TGA Q500 from TA Instruments equipped with an autosampler. The weight loss by heating the H-zeolites up

523 K at a heating rate of 1 $K.min^{-1}$ was considered to correspond to physically sorbed water.

Nitrogen-physisorption measurements were performed on a Micromeritics Instrument (Tristar 3000) at 77 K. Samples were degassed overnight under N_2 flow at 527 K prior to analysis. The specific surface area was calculated using the BET theory, while micropore volumes were estimated by the t-plot method.

Extraction of organic species from the zeolite

Organic species (other than the solvents) were analyzed on a spent zeolite by solid-liquid extraction on a Soxtec Avanti 2055 manual extraction unit. In a cellulosic holder, used zeolite catalyst was suspended and extracted according to the Randall method with refluxing dry acetonitrile (354 K), in immersion mode for 0.5 h and above the solvent for 2 h. Thereafter, excess solvent was evaporated and the extract analyzed by weighing and ^{1}H-NMR spectroscopy.

Re-use experiments

Re-use of zeolite catalysts in consecutive reactions in a high yield regime were carried out in o-xylene for 1h on a 50 wt% aqueous lactic acid solution with the oil bath at 443 K as described in the Methods section, but on a slightly larger scale (0.85 g of zeolite H-Beta (Si/Al 12.5) and adjusted amounts of other reagents) to allow for minor loss of material during handling. After analysis, the zeolite on the filter was dried at room temperature with the filter-setup vacuum, transferred to a porcelain crucible and calcined for 6 h at 823 K reached at a rate of 1 $K.min^{-1}$ in static air. Then, it was weighed and re-used with adjusted amounts of reagents in a consecutive run. These productive condition re-runs (around 80% of lactide yield) are seen as the series of light blue bars in Fig 3 of the main manuscript (5 re-uses, 6 reactions in total).

The re-use study was also conducted in the initial regime, to check for loss of activity. Due to very fast reaction kinetics in o-xylene, these experiments ran for 0.5 h with 0.125 g H-Beta (Si/Al 12.5) zeolite on 1.67 g of 50 wt% aqueous lactic acid solution in 10 ml solvent, with the oil bath at 443 K. This is necessary in order to study initial activities (<35% of lactide yield). Other procedures for re-use were identical as above for the productive regime re-runs. The initial regime re-runs are seen as the series of dark blue bars in Fig 3 of the main manuscript (5 re-uses, 6 reactions in total).

Custom zeolite Beta synthesis with large crystal sizes

In line with extensive literature, fluoride as a mineralizing agent in zeolite synthesis is known to lead to zeolites with large crystal sizes. For making a large crystallite H-Beta, synthesis was conducted using a literature recipe (*33*). More specifically, a gel with Si/Al ratio of 20 was obtained from tetraethylorthosilicate and metallic Al as respective Si and Al sources. Aqueous tetraethylammonium hydroxide was used as the organic structure-directing agent, while seeds of a commercial dealuminated Beta zeolite were added. After addition of HF (using appropriate safety precautions), the teflon liner was sealed in a Parr autoclave, residing for 12 days in a static oven at 413 K. After synthesis, the solids were filtered off, washed, dried and calcined at 773 K.

Supplementary Text

Large crystal size H-Beta experiment (Fig S12)

The zeolite-catalyzed production of lactide with a custom-H-Beta catalyst (with large crystallite sizes), under identical conditions shows a nearly identical kinetic plot as the commonly used commercial H-Beta (with very small crystallize sizes, Fig. S6). These observations further confirm that the reaction under these circumstances is running in the chemical regime and that the shape-selective product pattern of the zeolites is largely imposed by the intraporous acid sites, and not by external surface catalysis. The at least 30-times larger crystallites, having a much smaller external surface area (per weight) than the small particles of the commercial zeolite, still generate the same rate per weight of catalyst. The large crystal experiment thus confirms that the reaction rate under these conditions is limited by the chemical intraporous reaction and not by *e.g.* pore- or film-diffusional limitations. Additional information corroborating this is found in the high (and roughly similar) activation energies of the overall reaction and of the L_2A-to-lactide transformation (Fig S8). Diffusion-limited processes usually have much lower activation energies (*25*). The intermediate accumulation of the key intermediate, linear dimer (L_2A, Fig. 11B), also further suggests that the reaction is running in the chemical regime of ring-closing condensation. The high activation energy values in toluene are confirmed by the much faster reaction in xylene due to its higher boiling point and thus reflux reaction temperature (417 K, Fig S7). Using the E_A value in toluene (356-384 K), a 6.6 increase in the reaction rate is expected if experiments would be performed in toluene boiling at 417 K (using increased pressure). The reaction rate increase in o-xylene (6.3-fold increase w.r.t. toluene, Fig S11A) is correctly predicted by the high apparent activation energy, derived from toluene experiments at varying pressures (and thus reflux reaction temperatures). This suggests that the nature of the (aromatic) solvent is not really affecting the catalytic reaction rate.

Zeolite post-run extraction

After a 3 h of reaction (oil-bath at 403 K) with 3.32 g of 50 wt% L-LA solution, 1 g of H-Beta (Si/Al 75) and 20 mL of toluene, the zeolite was collected during the classic work-up of the reaction mixture, and subjected to solid-liquid extraction in acetonitrile (see Methods). 90 mg of organic carbon was extracted (all lactyl species). Analysis via ^{1}H-NMR showed that this fraction has the following distribution: 4% lactide, 36% LA and 58% lactyl oligomers (L_nA, $n \geq 2$) with a number average length of 3.0. After extraction and solvent drying, 1.01 g of zeolite (essentially free of carbon) was recovered.

Calculating Weisz' shape-selectivity factor

According to Weisz, the degree of shape-selectivity S is the ratio of the appropriate observed effective rates or rate constants, as compared to their usual ratio in the absence of structural constraints on molecular motion: $S = (k'_p/k'_a)/(k_p/k_a)$, with k_p/k_a the ratio of the intrinsic rate constants in the absence of spatial constraints (*20*).

In our case, in absence of zeolite (auto-catalyzed blanc reaction, with water-removal set-up) the ratio of rate-constants, $k_a/k_p = 0.53$ (with a = lactide and p = L_nA with n > 3). In presence of H-Beta (Si/Al 12.5), the rate ratio $k'_p/k'_a = 3.98$. The shape-selectivity factor thus mounts to 7.5, which is clearly larger than 1 (shape-selectivity if > 1). Comparing to soluble acids for rates in the case of non-constrained environment (but with acid catalyst) even larger factors are attained. (Reactions with oil bath at 413 K, 50 wt% aqueous LA feed, with and without 0.5 g of zeolite, 1.67 g of L-LA (50 wt%), 10 mL toluene).

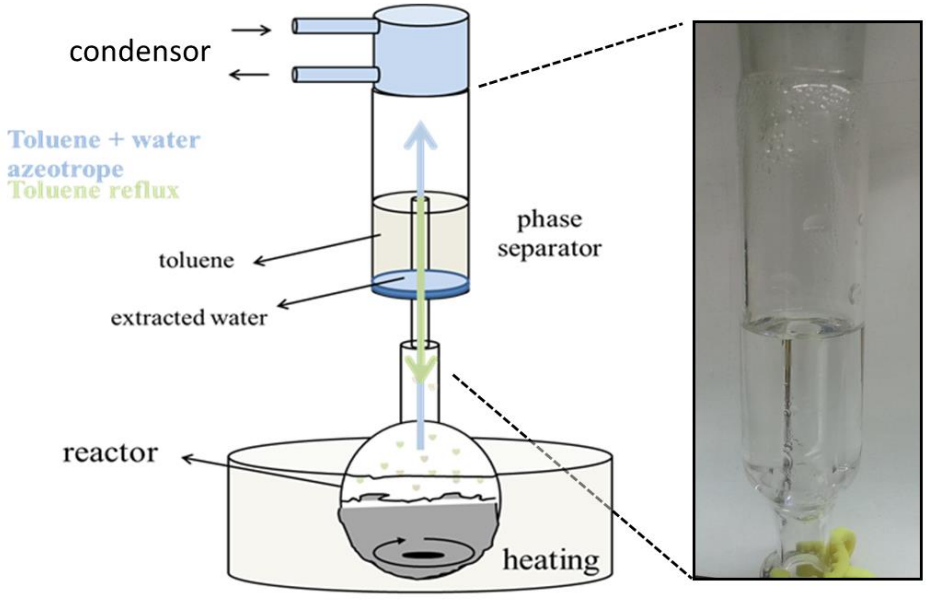

Fig. S1.

General lab-scale setup for catalytic reactions. The scheme on the left shows the small scale reactive distillation setup with condenser and phase-separator for water-removal, resembling a Dean-Stark operation. Whereas a Dean-Stark setup usually runs an azeotropic distillation at the temperature of the azeotrope, here, entraining of water is achieved at the boiling point of the reflux solvent (see Fig S7). The unique part of the setup is the phase-separation unit (image right of the scheme), as designed by the authors and produced in a glass workshop of KU Leuven. With this setup, it is possible to achieve accurate results for reactive distillation reactions where water needs to be continuously removed at a scale as small as 10 mL of reaction volume. This unit allows to measure reproducible catalyst behavior, solvent and substrate screening, as well as kinetic behavior. Setups scaled-up to 50 mL in volume (slightly modified) were producing identical results.

A)

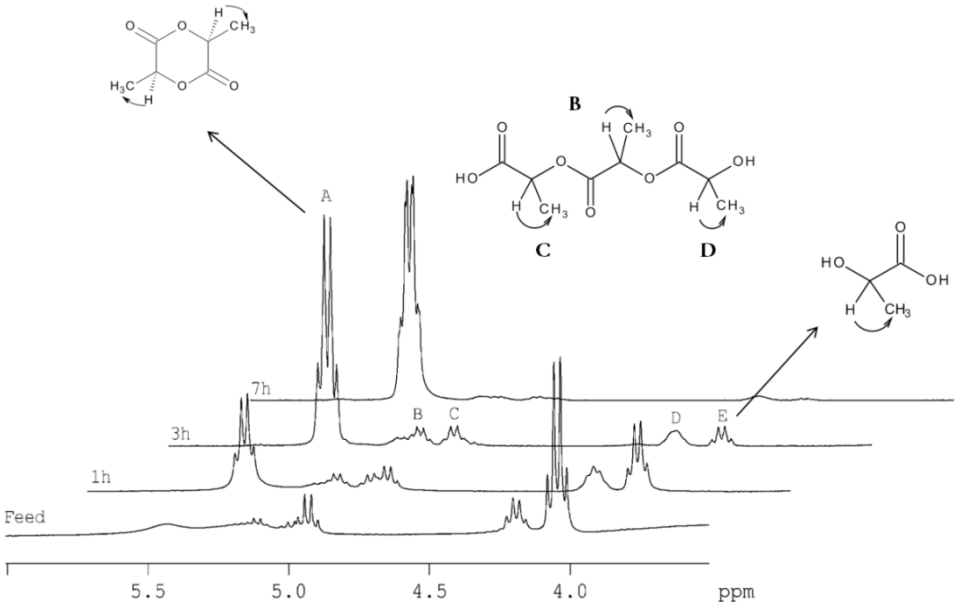

B)

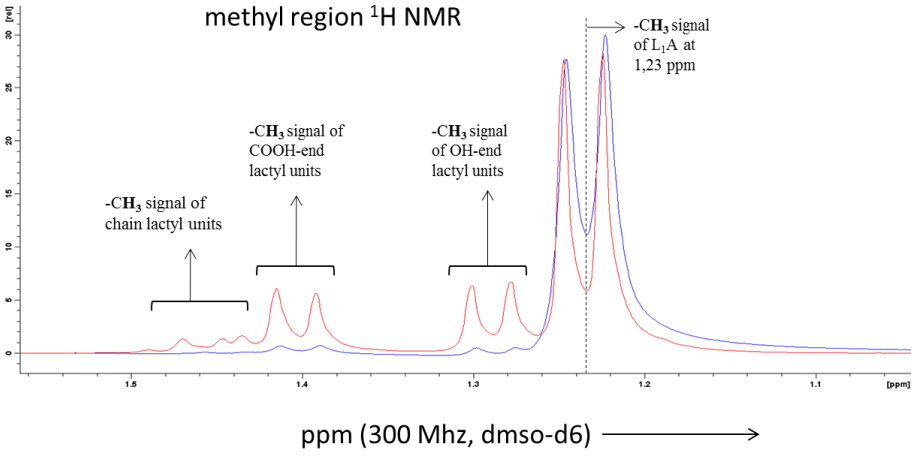

Fig. S2.

Typical ^{1}H-NMR analysis in DMSO-d6. A) The methine [-C**H**-CH$_3$] quartet region of a series of reaction mixtures. Methine proton signals of A: lactide, B: centers of oligomers, C: carboxylic end groups of oligomers. D: hydroxyl end groups of oligomers, and E: lactic acid are assigned. Conditions of the reaction: 0.5 g of H-Beta (Si/Al = 12.5), 1 g of L-lactic acid solution (90 wt%), oil bath at 403 K, 10 mL toluene, samples of 3 different reactions quenched at indicated time intervals. **B)** Shows a comparison of 50 wt% (blue) and 90 wt% (red) LA solutions in the methyl [-CH-C**H$_3$**] doublet region.

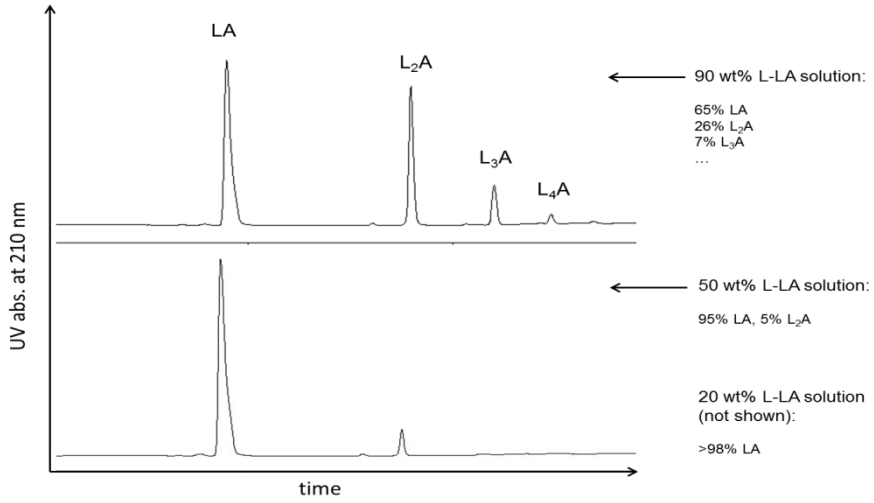

Fig. S3.

Typical HPLC analysis comparing two aqueous L-LA feedstock solutions: 50 wt% (bottom) and 90 wt% (top).

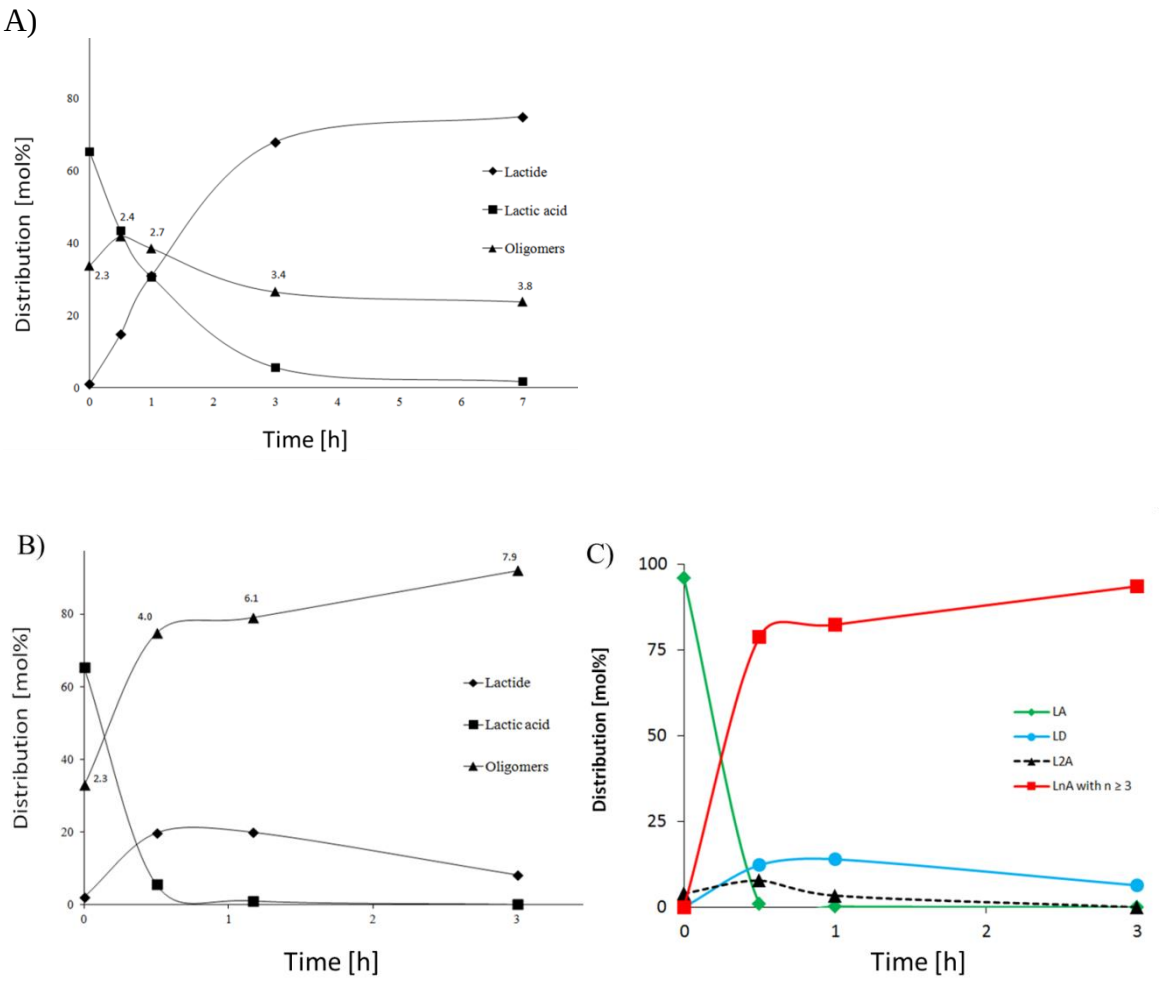

Fig. S4.

Additional time profiles of catalytic reactions: A) With a shape-selective zeolite (non-optimal conditions) on a 90 wt% LA-solution as feed. Conditions: 0.5 g of H-Beta (Si/Al = 12.5), 1 g of L-lactic acid solution, temperature oil bath at 403 K, 10 mL toluene. Labels indicate the number average length of the oligomer fraction (L_nA, w ith $n \geq 2$). This feedstock clearly contains oligomers (mainly L_2A and L_3A) from the start. **B)** With a non-shape-selective catalyst in the same conditions as in A, but instead of zeolite, with homogeneous acid catalyst H_2SO_4 (0.01 g). The lactide yield is always lower than 20 % with H_2SO_4. **C)** With a non-shape-selective catalyst (H_2SO_4) on 1.67 g of a 50 wt% aq. LA solution, temperature oil bath at 413 K in 10 mL of toluene. This time plot can be compared with Fig 2D in the main manuscript as it is performed in identical conditions with the same amount of proton acidity added (here from H_2SO_4). LD = lactide. Deconvolution of L_2A from OLA fraction via HPLC. Such unselective patterns are in line with literature on PLA synthesis by polycondensation (*34*, *35*).

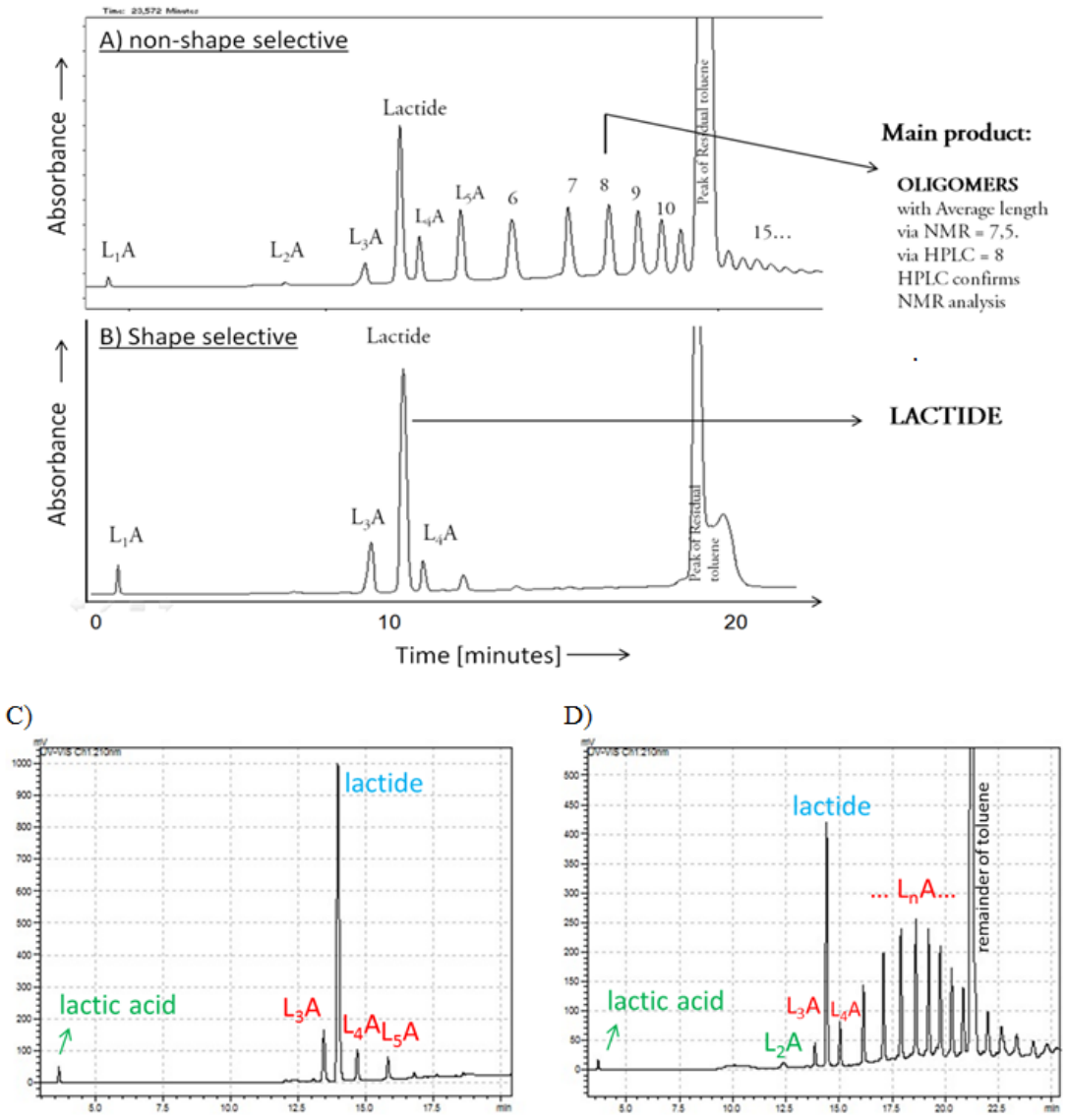

Fig. S5.

Full HPLC profiles of reaction products formed in reactions with: **A)** a non-shape-selective resin catalyst on a 90 wt% aqueous LA feed: 0.25 g of Amberlyst 15 wet, 1 g of L-lactic acid solution (90wt%), 403 K, 10 mL toluene, 3h. **B)** the shape-selective H-Beta zeolite on a 90 wt% aqueous LA feed. 0.5 g of H-Beta (Si/Al =12.5), 1 g of L-lactic acid solution (90 wt%), 403 K, 10 mL toluene, 3h. **C)** a shape-selective catalyst. This is a zoom-out of the HPLC profile in Fig 2C in the main manuscript for the selective zeolite H-Beta Si/Al 12.5 catalyst: 50 wt% aqueous LA feed, 0.5 g of zeolite, 1.67 g of L-LA (50 wt%), oil bath 413 K, 10 mL toluene, 3h. **D)** a non-shape-selective catalyst: 0.25 g of wet Amberlyst 15, in conditions of C. The right frame in Fig. 2C in the main manuscript is performed in identical conditions with NAFION resin (0.61 g). Figures S5C and S5D and Fig 2C (right frame) are thus compared at equal (nearly full) LA conversion reached with an equal amount of acid sites added.

A)

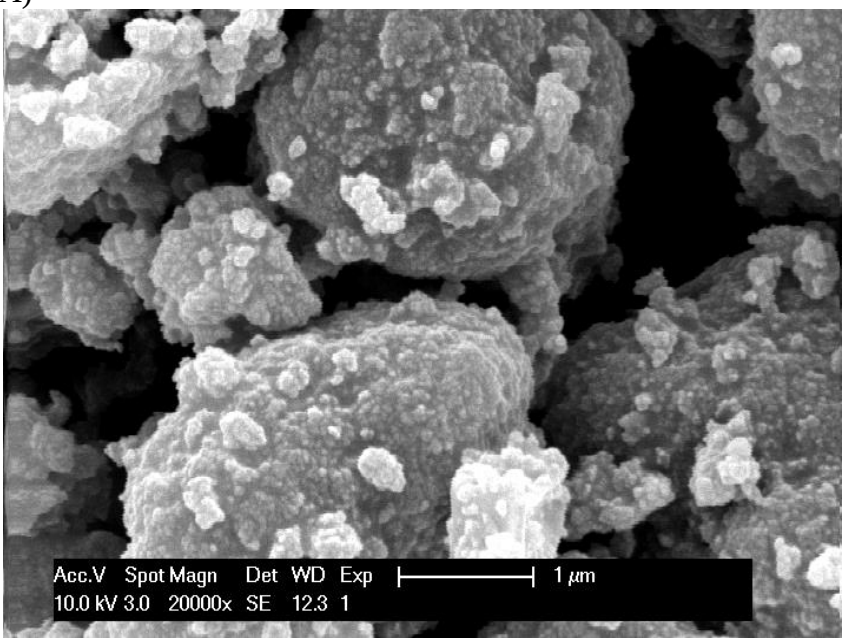

B)

12 T-atom membered zeolite ring
(e.g. BEA topology: H-Al-Beta, pore diameter 0.595 nm;
largest sphere that can be included: 0.668 nm)

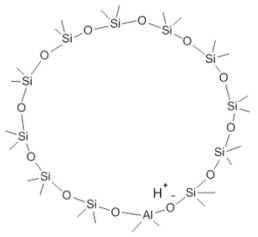

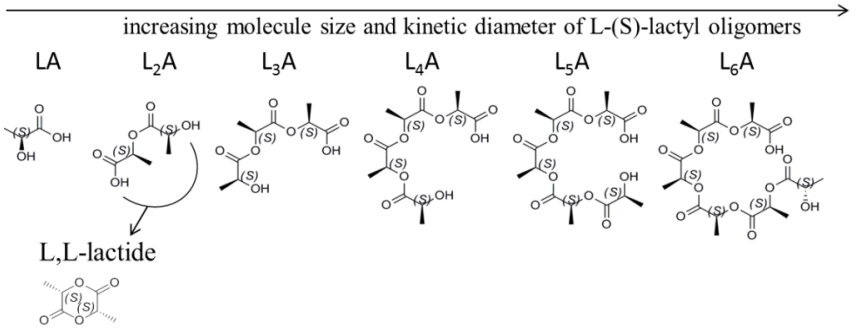

Fig. S6.

A) SEM photograph of the used H-Beta Si/Al = 12.5 zeolite. These are aggregates of smaller nano-sized crystallites of about 10-30 (<50) nm in diameter. This is typical for commercial Beta zeolites made in hydroxide media. More detailed information on the (size) properties of this commercially available catalyst can be found in (*36*), a publication that made use of exactly the same batch of catalyst. **B)** Tentative comparison of the pore size of a 12 T-atom membered ring zeolite (BEA) and increasing sizes of L-lactic acid, cyclic L,L-lactide, linear dimer and oligomers of L-lactic acid (L_nA).

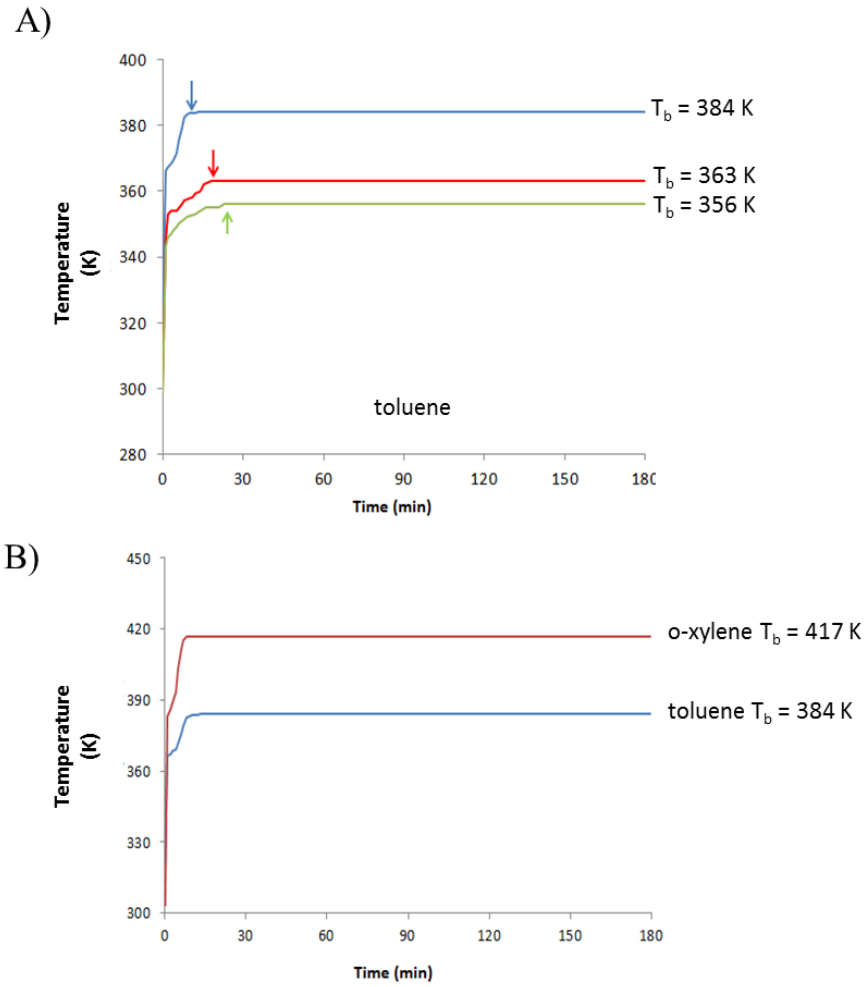

Fig. S7.

Temperature-time profiles of zeolite reactions: A) in toluene at different boiling points. As we usually start from 1.66 g of a 50 wt% LA solution, in 10 mL toluene, the initial mixture will contain 0.83mL H_2O. At the start of the reaction, the reactor is submerged in a pre-heated oil-bath (at 403 K, 383K and 376 K for the decreasing pressures used in toluene). The temperature-time profiles of zeolite reactions performed at 384 K (atmospheric pressure), 363 K (530 mbar) and 356 K (395 mbar) are given. As can be seen, the boiling point of the solvent (T_b), *i.e.* the actual reaction temperature in the refluxing solvent system, is reached in the very initial phase of the reaction. The time necessary to reach T_b is shorter, if the boiling point is higher. The actual reaction temperature is reached (indicated with the arrows) after 9 min at T_b = 384 K (atmospheric pressure), 18 min at T_b = 363 K (530 mbar) and 23 min at T_b = 356 K (395 mbar). **B)** in o-xylene (compared to toluene of Fig 7A) at atmospheric pressure. Temperature of the pre-heated oil-bath is 443 K. Time to reach T_b in o-xylene (417 K) is 7 min.

A)

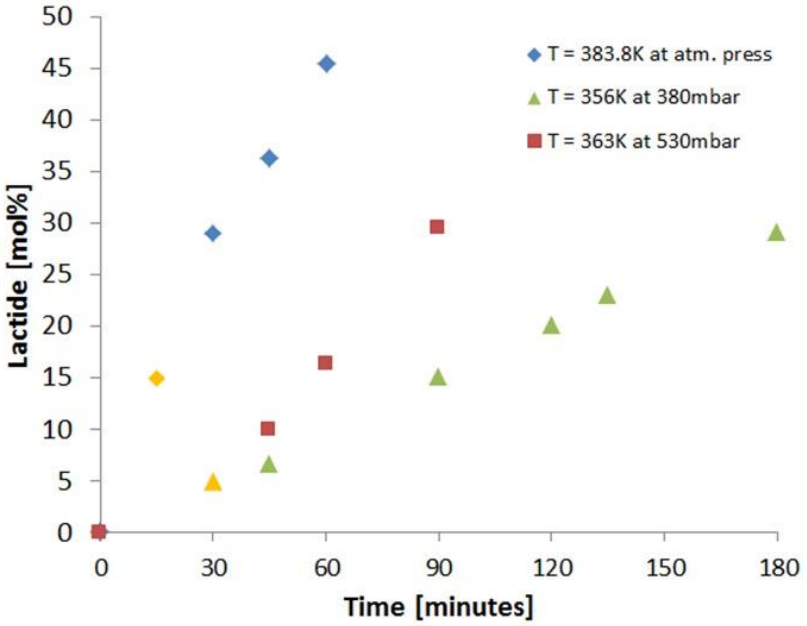
T = 383.8K at atm. press
T = 356K at 380mbar
T = 363K at 530mbar
Lactide [mol%]
Time [minutes]
0
5
10
15
20
25
30
35
40
45
50
0
30
60
90
120
150
180

B)

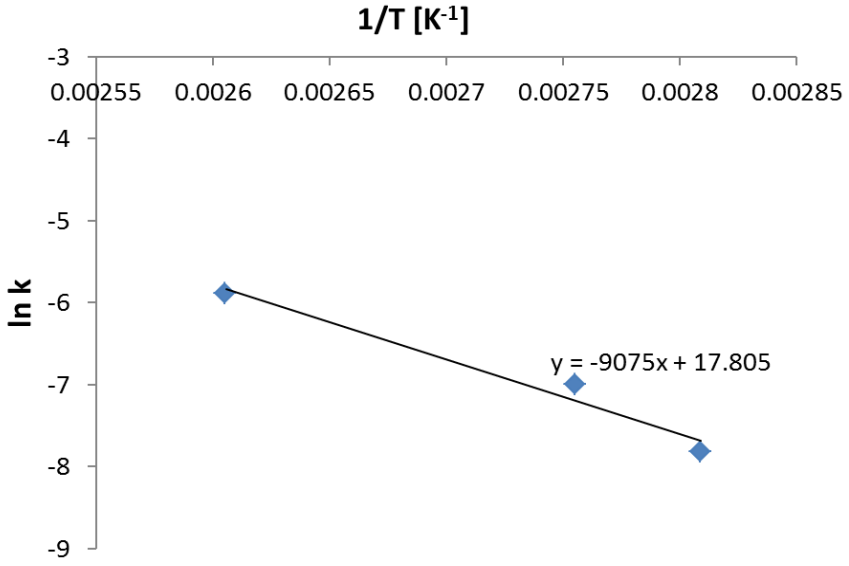
1/T [K-1]
ln k
y = -9075x + 17.805
-3
-4
-5
-6
-7
-8
-9
0.00255
0.0026
0.00265
0.0027
0.00275
0.0028
0.00285

C)

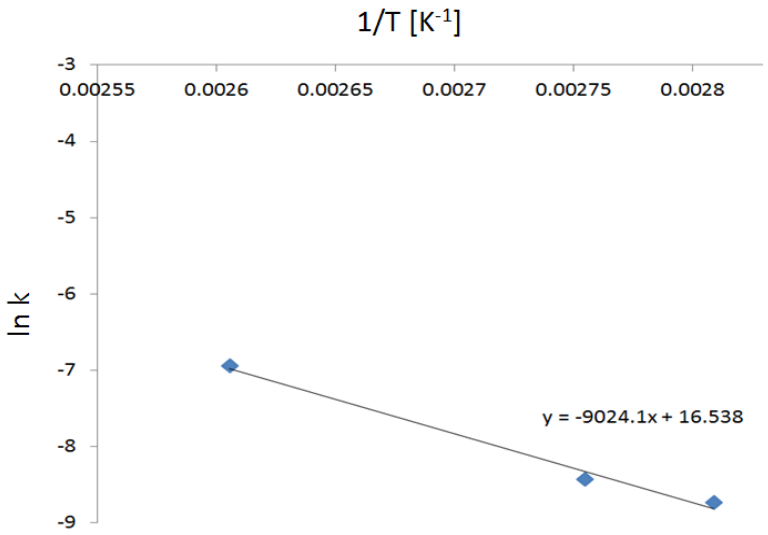

Fig. S8.

Determination of apparent activation energies of H-Beta catalyzed reactions. A) Initial kinetics of the overall reaction under reduced pressures. Conditions: 0.83 g L-LA (1.66 g 50 wt% aqueous solution); 0.5 g of H-Beta (Si/Al 75); 10 mL of toluene, reactions at 356, 363 and 384 K.). Orange points, tentatively indicated on the plot for comparison, were performed by using half the amount of catalyst, while applying a double reaction time. In this way, a shorter reaction is simulated (with 0.5 g), while initial transient time (= time to reach the boiling point, Fig. S7A) can be neglected compared with the time of sampling. These points follow the linear behavior of both plots. Further evidence of kinetic viability in Fig. S9A. The rates were extracted from the initial linear regime. The 30 minute reactions were evaluated in duplicate, resulting in very similar lactide kinetics. One can see in the time-temperature plots of Fig S7A that the short times to reach the boiling points, are small compared to the time of determined kinetic data at low pressures. Note that intermediate sampling is not performed (see analysis section), and that every kinetic point is determined by running individual reactions. **B)** The Arrhenius plot for the overall reaction: LA to lactide based on rates from (A). Units of k = $mol_{lactide}.h^{-1}$ and the resulting apparent activation energy for this overall reaction: 75.4 kJ/mol. **C)** The Arrhenius plot for the L_2A (linear dimer) to lactide reaction by experiments under reduced pressures. Conditions: 0.3 g (L-)L_2A, 0.1 g of H-Beta (Si/Al 75); 4 mL of toluene, reactions at 356, 363 and 384 K. Kinetics assessed < 36% of lactide yields for all three temperatures and extrapolated through zero. Units of k = $mol_{lactide}.min^{-1}$. Apparent activation energy for this L_2A to lactide reaction: 75.0 kJ/mol.

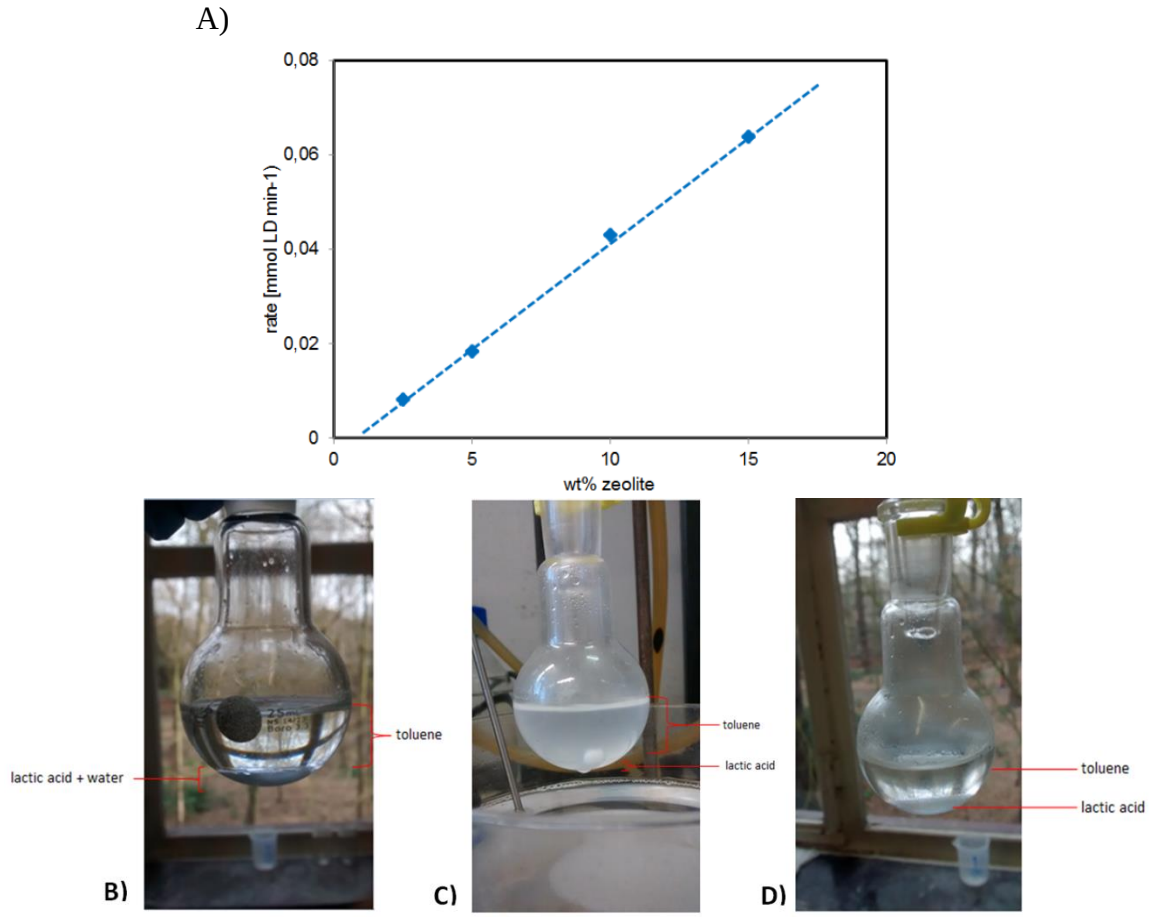

Fig. S9.

Initial kinetics assessed with different amounts of catalysts and state of lactic acid during reaction. A) The melting point of L-lactic acid is 325.8 K. Due to its very high hygroscopic behavior, lactic acid is commercially and practically mostly encountered in aqueous solutions. In the reaction conditions, at temperatures well above the melting point, we are dealing with an emulsion of lactic acid (and initially water) and toluene, as lactic acid is poorly soluble in these solvents. Such emulsified state could affect the kinetics, for instance on the transfer of LA across the two liquid states. Therefore, a set of catalytic reactions was carried out with varying amounts of catalyst, in the initial rate regime (Fig S9A). Clearly, a linear relationship is obtained, suggesting that the emulsifying conditions are not governing the reaction rate and molecular transport is not rate-determining in the conditions tested. Determination of apparent kinetic parameters is therefore allowed despite the emulsifying reaction mixture. Conditions: toluene, oil bath at 403 K, 1.66 g of a 50 wt% LA solution. Weight % of air-equilibrated zeolite (H-Beta Si/Al 12.5) versus total weight of lactic acid, zeolite and solvent. **B-D)** Pictures of reaction mixtures (conducted in absence of zeolite). Before the start of the reaction (9B), an emulsion of a toluene phase and a water/lactic acid phase is observed. Directly after a blanc reaction at 384 K, a somewhat turbid mixture is observed (9C), while the mixture still consists of 2 phases. After 3 h, (9D) the biphase was settled.

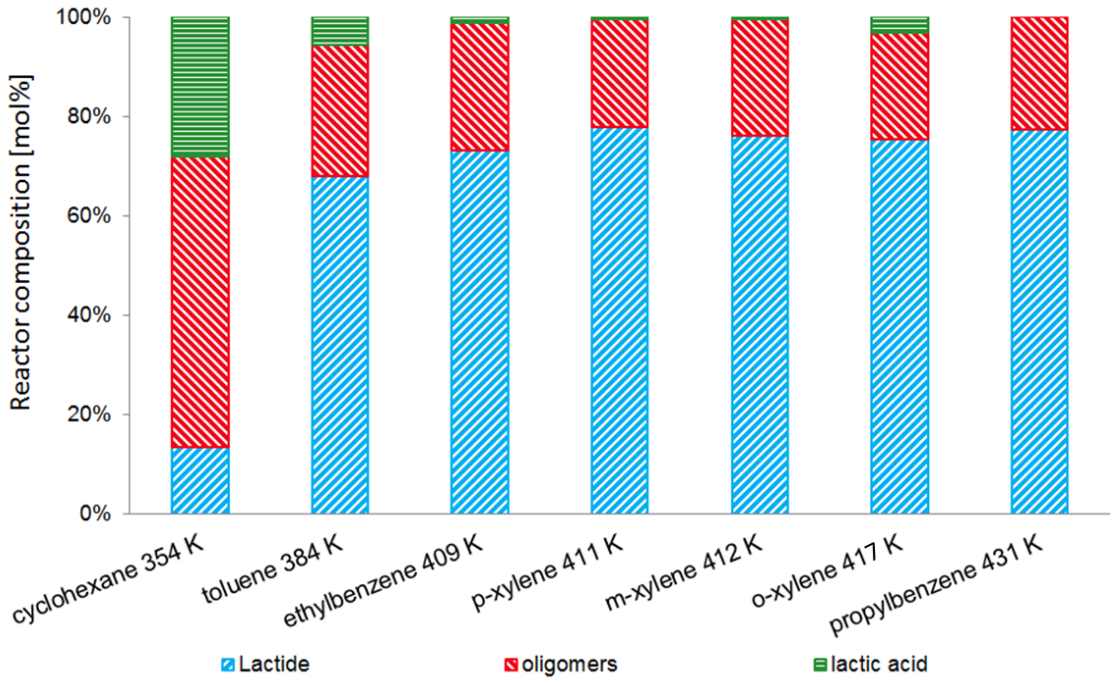

Fig. S10.

Preliminary solvent screening for the zeolite catalyzed conversion of LA with H-Beta (Si/Al 12.5). The boiling point (T_b) of each solvent is indicated in the figure. The heating input of the oil bath was set at T_b + 20 K. Reaction on 1 g of L-LA 90 wt% (non-optimal feedstock, see Fig S16) with 0.5 g of zeolite for 3 h. The process is relatively flexible in (aromatic) solvent choice. Data and kinetics in optimal conditions for o-xylene are found in Fig S11 and in the main manuscript.

A)

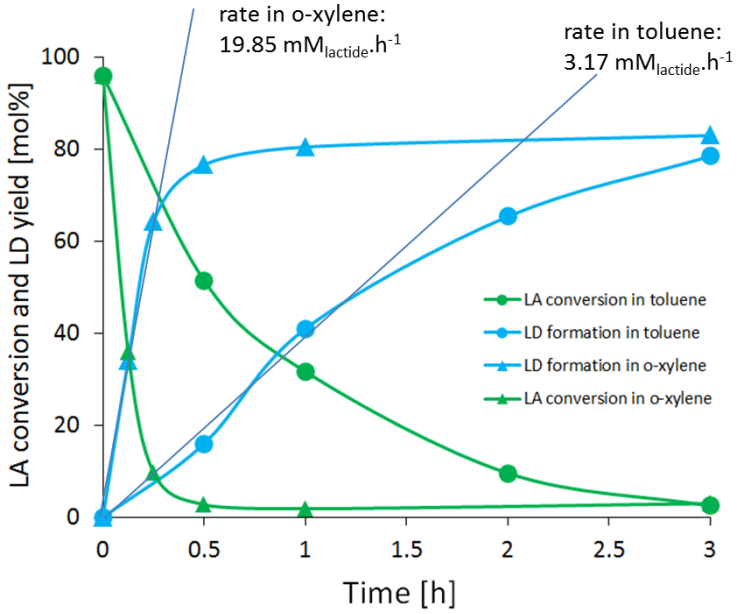

B)

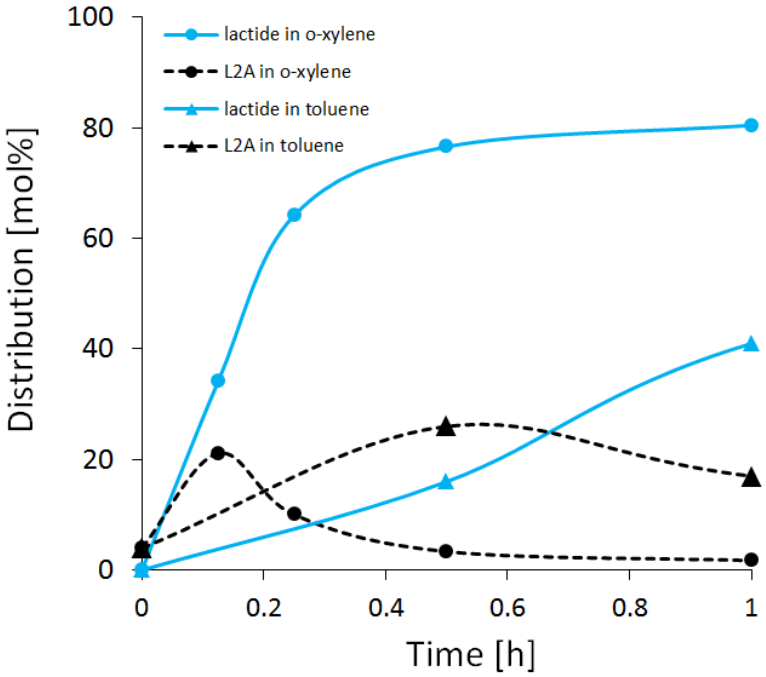

Fig. S11.

Kinetics of the reaction with H-Beta (Si/Al 12.5) in o-xylene compared to toluene. **A)** Comparison of lactide yield and LA conversion. 1.67 g of L-LA 50 wt%, 0.5 g of zeolite in 10 mL of solvent. Temperature of the oil bath: 413 K for toluene and 443 K for o-xylene. LD = lactide. **B)** Comparison of the L_2A formation in o-xylene compared to toluene. Note how the L_2A (key intermediate) maximum is shifted to shorter contact times, and also lower in o-xylene (20 %) compared to in toluene (26 %). Reaction temperature in o-xylene is 417 K, in toluene, 384 K (see Fig S7).

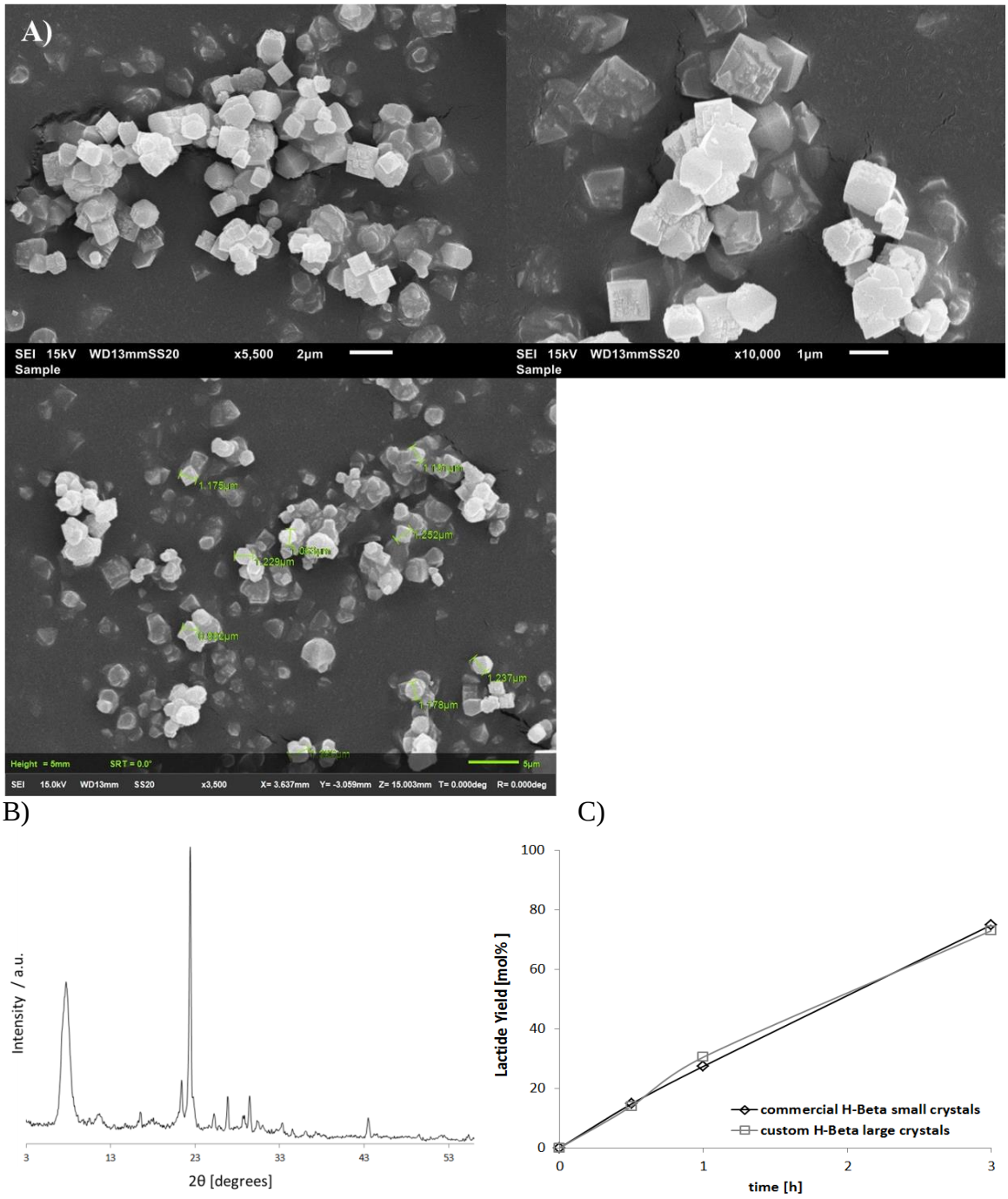

Fig. S12.

Custom H-Beta (large crystals) characterization and reaction testing. A) SEM imaging of the crystallites. Crystals size in the 1-1.5 µm range, at least 30 times larger than the commercial Beta catalysts (from classic hydroxide mediated routes). **B)** Powder X-ray analysis showing *BEA topology (*37*). The Si/Al ratio of the zeolite was determined to be 17 by ICP-AES. **C)** Lactide formation kinetics with H-Beta with commercial small and custom large crystallite sizes. 1.67 g of L-LA 50 wt%, 0.5 g zeolite, 10 mL toluene, oil bath temperature of 403 K.

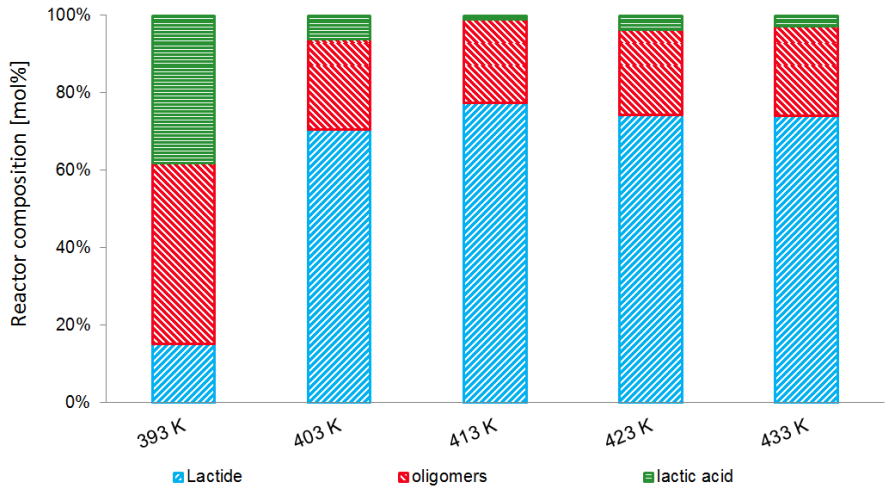

Fig. S13.

Influence of the heating input (T of the oil-bath) of the reactor on the reaction in toluene. 1.66 g of L-LA (aq. 50 wt%), 0.5 g H-Beta (Si/Al 12.5), 10 mL of toluene, 3 h. (actual reaction temperature = boiling point 384 K, see Fig. S7). Oil bath at 393 K is not efficient for lactide formation. Another experiment with a two-neck round bottom flask was performed under identical conditions of the 413 K experiment in Fig S13, but instead of letting the toluene reflux, the phase-settler trap was emptied each time when nearly full and simultaneously, the reaction volume in the flask was kept constant by continuous addition of fresh (not-water saturated) toluene through a septum via the second arm of the flask. This afforded a yield of 85 mol% of lactide, versus 78.5 mol% when water-saturated toluene refluxes. Industrially, this points to the need of efficiently engineering and controlling the water-removal via reflux distillation (also see Table S1).

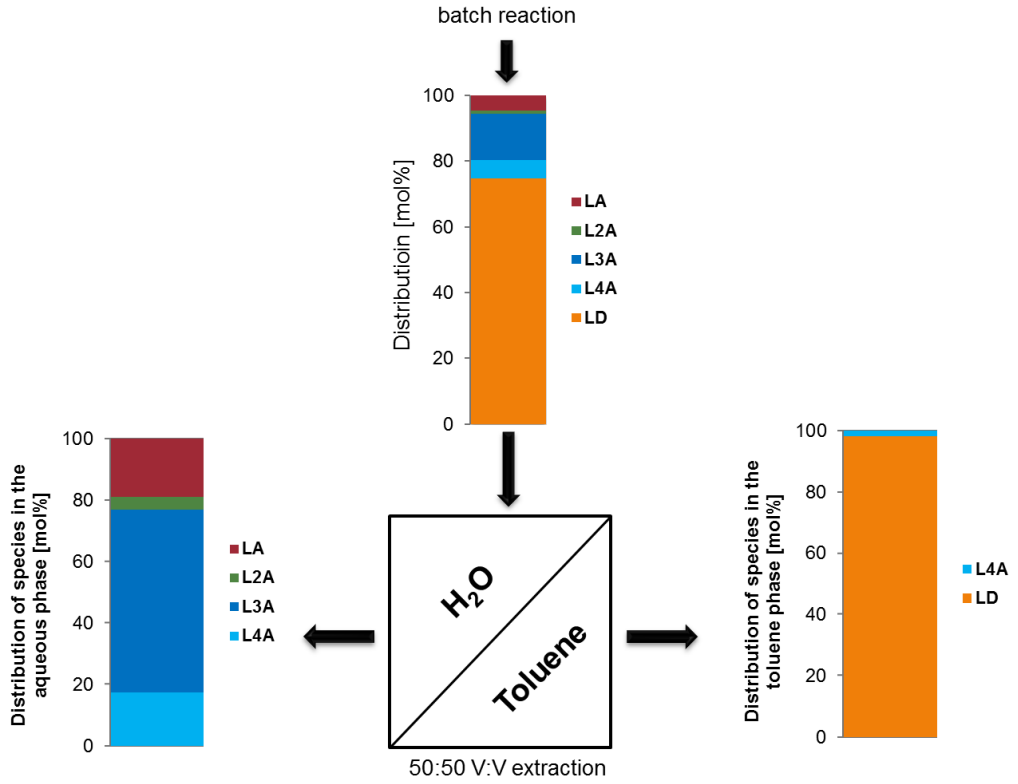

Fig. S14.

Liquid-liquid extraction of an actual reaction mixture (LD = lactide). Conditions: 1.67 g of L-LA (aq. 50 wt%), 0.5 g H-Beta (Si/Al 12.5), 10 mL of toluene, 3 h. Heating input (oil bath) at 403 K. After classic work-up (methods) the total reaction mixture was fully dried to get rid of the acetonitrile and subjected to a toluene: water (both 5 mL) liquid-liquid extraction by simple stirring and gravitational phase settling. Both phases were analyzed by ^{1}H-NMR and HPLC for individual oligomer analysis. The distribution of oligomers clearly shows that LA, L_2A, L_3A and L_4A prefer the water phase. L_4A is the first oligomer to be minimally dissolved in the organic phase, whereas L_5A is not formed by the zeolite in this reaction. Lactide prefers the organic phase. The relative distribution of oligomers and LA in the aqueous phase differs slightly from their distribution in the reaction mixture. This is indicative of an already spontaneous occurring hydrolysis of short oligomers to lactic acid due to the excess of water in the extracted aqueous phase over time. This indicates the easy recovery and recycling of the short oligomers of lactic acid, the only side-products of the zeolitic reaction. They can be easily extracted and hydrolyzed back to LA (*e.g.* in R2 in main manuscript, Fig 3). This hydrolysis is spontaneous and complete in excess water and can be accelerated with an acid catalyst or heat (*14*). Such hydrolyzed oligomer stream (LA-L_2A) is ready for re-insertion in the process' main reactor (R1). As longer and more apolar oligomers (preferring organic phases) are not formed due to the zeolite's shape-selective behavior, minimal downstream processing via liquid-liquid extraction (ideally, with removed condensation water from P1 in Fig 3) and catalytic reaction are in a perfect balance. Another complementarity is encountered in the ease of lactide recovery from the organic solvent (Fig S15).

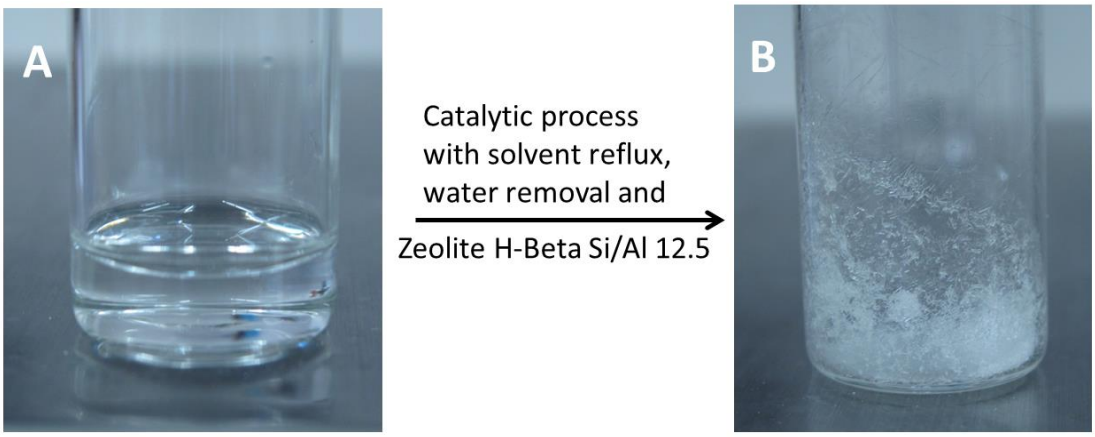

Fig. S15.

Spontaneous crystallization of lactide after solvent evaporation. A) Aqueous lactic acid solution before reaction; **B)** entire reaction mixture after zeolite and solvent removal (see work-up) of an 85 % lactide yielding reaction in toluene (85 % pure in lactide). After liquid-liquid extraction, *viz*. Fig. S14, 98 % purity can be achieved (^{1}H-NMR). These solvents are widely used recrystallization media for cyclic esters (*e.g.* prior to lactide polymerization in solvent or bulk) (*38*, *39*). The complementarity between the use of these solvents in the main reaction of the process (for removing water and dissolving lactide) and the ease of lactide crystallization (and solvent recycle) is obvious.

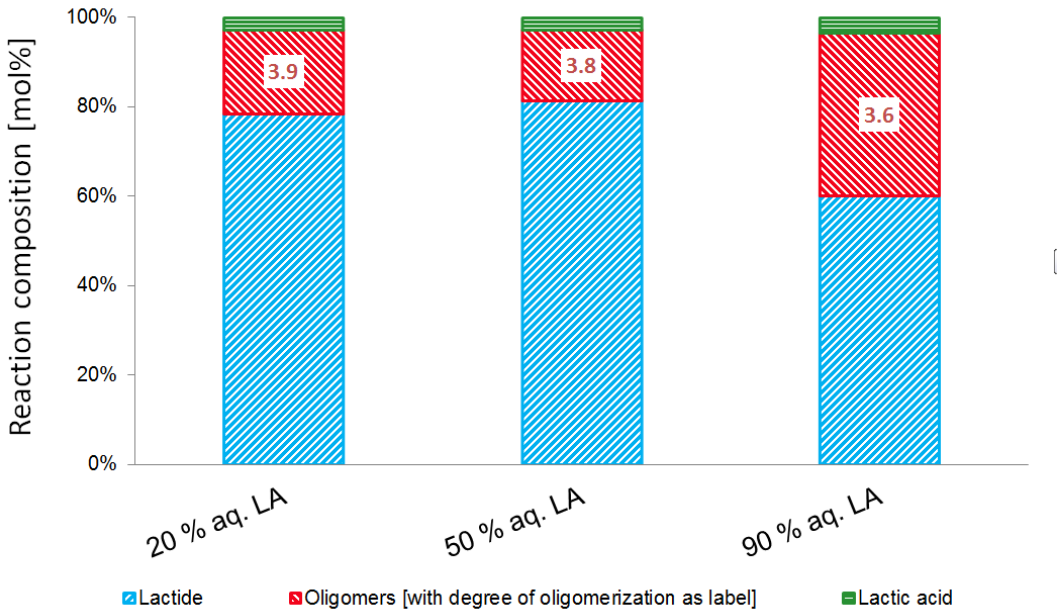

Fig. S16.

Variation in the amount of water in the aqueous lactic acid feed: 20, 50 and 90 wt% LA in water solutions. Lactic acid to solvent ratio held constant. Conditions: 4.18 g of L-LA (aq. 20 wt%) or 1.67 g of L-LA (aq. 50 wt%) or 1 g of (aq. 90 wt%) with 0.5 g H-Beta (Si/Al 12.5), 10 mL of o-xylene, 1 h. Heating input (oil bath) at 443 K. Labels indicate the number average length of the oligomer fraction (L_nA, with $n \geq 2$). The composition of the 3 feedstocks differs greatly as tabulated in (*14*) and explained in the section Methods (and Figs S2B, S3). There is virtually no influence of the amount of water on the conversion of LA. Compared to the 20 wt% aqueous LA solutions, the amount of added physical water from the 50 wt% feedstock is 4 times greater. Due to the solvent distillation and fast water-removal, no difference in products and selectivity is found here, indicating that the process is flexible in terms of lactic acid feedstock. In the case of 90 wt% solutions, the yield is reduced, however. This is due to the fact that equilibrated (*e.g.* commercial) lactic acid solutions that are highly concentrated contain up to 35 % of oligomers of lactic acid (mainly dimer, trimer and tetramer) due to autocatalyzed self-condensation equilibria. Towards industrial scale-up, the prospect of using more diluted aqueous LA feedstocks is more appealing, because the output of the fermentative production of LA is rather diluted.

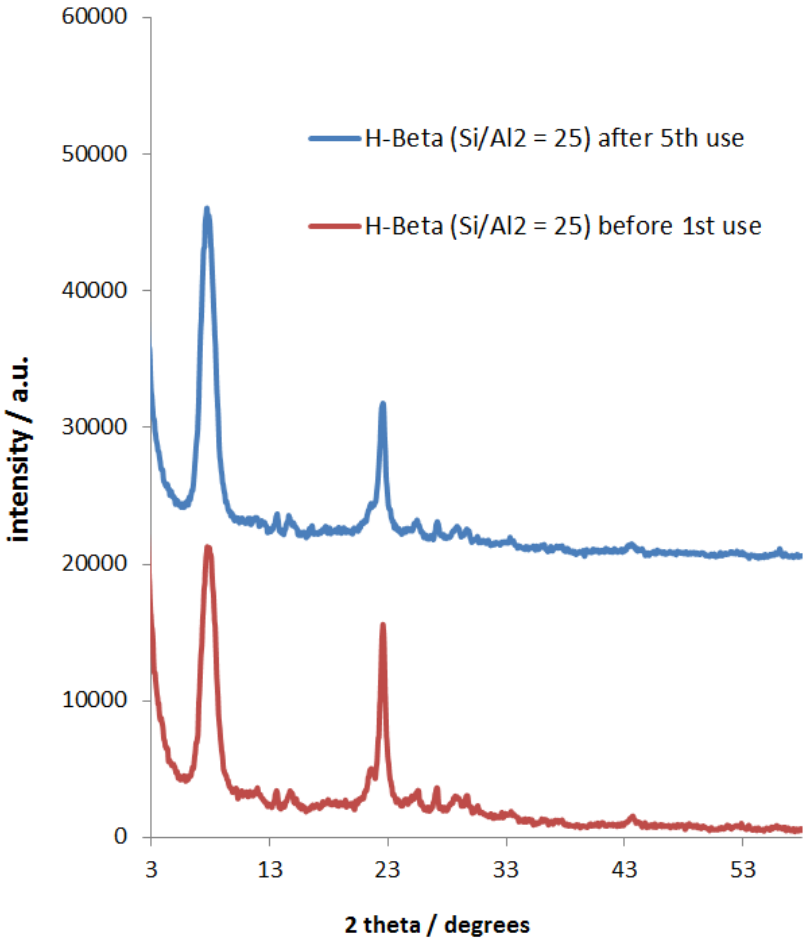

Fig. S17.

PXRD of the zeolite before the 1st and after the 5th experiment in the re-use study. No significant differences in the degree of crystallinity was noticed between PXRD patterns before the first and after the 5th run (productive re-run conditions). The BEA topology is intact even after 5 catalytic runs and the zeolite keeps on working during the 6th run, exactly as in the 1st run (catalytic results of re-use study are found in Figure 3 in the main manuscript, both in initial and productive regime). The Si/Al ratio after the 6th use was determined by ICP/AES analysis and was found to be 13.2. This is very close to the Si/Al value of the fresh catalyst (12.9) and within experimental error. This confirms the virtual absence of Al leaching and disappearance of active sites.

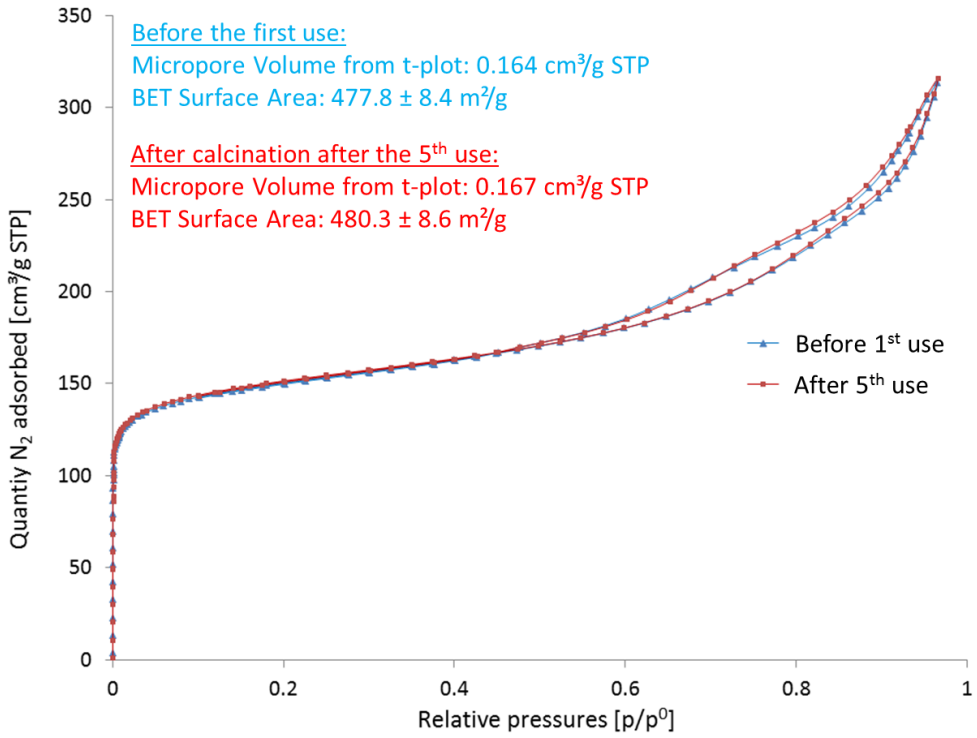

Fig. S18.

Nitrogen physisorption isotherm on the H-Beta zeolite before the 1st and after the 5th use in the re-use study (productive conditions). The catalyst has not changed structurally (similar pore volume and BET surface area) nor activity/selectivity-wise (Fig. 3 in main manuscript) and is stable in the process conditions (o-xylene boiling at 417 K).

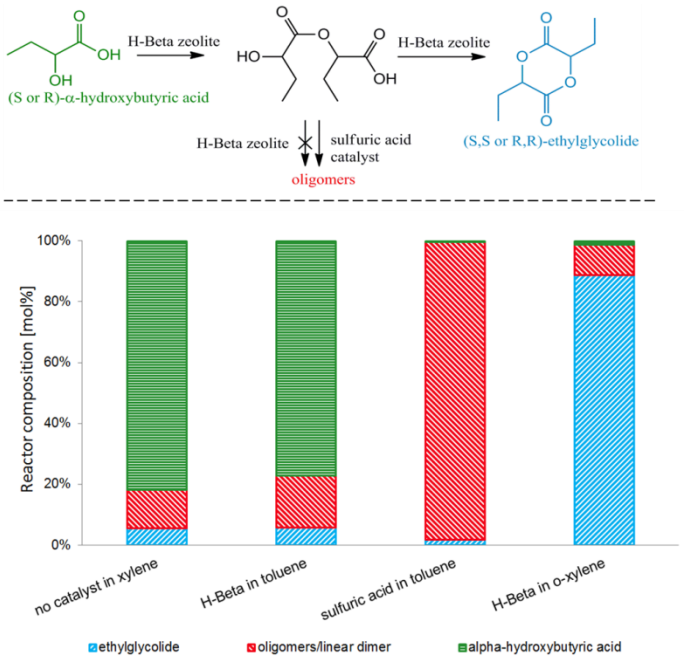

Fig. S19.

Reaction path and results for the shape-selective cyclic dimerization of α-hydroxybutyric acid and α-hydroxybutenoic acid. Experimental conditions: 0.5 g of D (or R)-α-hydroxybutryic acid; 0.5 g of zeolite or 0.030 g in case of H_2SO_4. Temperature of oil-bath at 413 K for toluene and 443 K for xylene, 3 h of reaction. Distribution based on ^{1}H-NMR yield analysis similar to LA analysis, while ethylglycolide yield was confirmed by gas chromatography using an external standard and the effective carbon number method method (*40*). As reaction with the zeolite in toluene (384 K) did not show much condensation activity, the reaction was carried out in refluxing o-xylene at higher temperature. In line with lactide formation from LA, the shape-selective formation of cyclic dimer (EG) from the monomeric acid can thus be catalyzed with zeolites in high yields (up to 88%), whereas sulfuric acid, as soluble catalyst, yielded only oligomers. A reaction without catalyst did not produce significant EG yields either. The straightforward protocol avoids use of cumbersome multistep procedures such as described for the synthesis of ethylglycolide, the precursor for poly-2-hydroxy-butyrate via ring-opening polymerization (*41*). Though these polymers might possess interesting properties, the reported routes for dimer synthesis is very impractical. For the synthesis of vinylglycolide from rac-α-hydroxybutenoic acid in o-xylene in identical conditions, only 16 % of cyclic dimer was obtained due to the occurrence of side reactions such as aromatic ring alkylation with the vinyl side group. Analysis was done with GC and external standard, based on the effective carbon number method (*39*), due to absence of a commercial vinylglycolide standard. Alkylated aromatic ring products were analyzed with GC-MS. In milder conditions, *viz.* in toluene (384 K boiling point, heating oil bath at 403 K) for longer reaction times (24h), an improved 24 % cyclic ester yield was found.

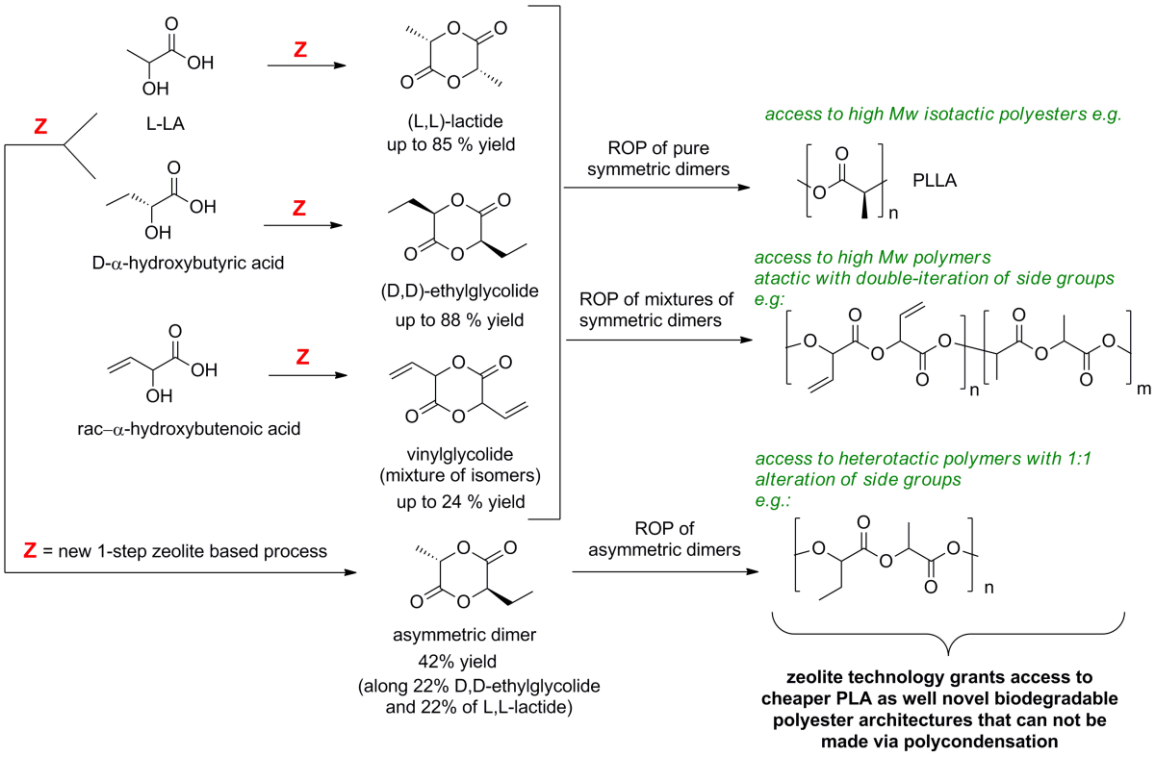

Fig. S20

Preliminary assessment of the substrate scope of the zeolite-based process. Tentatively, some (novel) polymer architectures are drawn, the formation of which should be facilitated by this new route to cyclic dimers. Results for the zeolite-catalyzed mixed-monomer dimerization of D-α-hydroxybutyric acid and L-LA are indicated (o-xylene, oil-bath at 443 K, 0.5 g of H-Beta (Si/Al 12.5), 3 h, equimolar mix of acid feedstock, ^{1}H-NMR analysis). The resulting functional asymmetric dimer (42 % yield) is hereby accessible in a single reaction step.

Table S1.

Additional reaction results[a]

entry	catalyst	LA substrate (wt%)	lactide yield [mol%]	LA [mol%]	oligomers [mol%]
1	-	90[b]	8	48	44
2	H-Beta Si/Al 12.5	90	68[c]	5	27
3	H-Beta Si/Al 180	90	12	49	39
4	NH_4-Beta Si/Al 12.5	90	18	49	33
5	H-Beta Si/Al 12.5	L_2A[d]	93	0	7
6[e]	H-Beta Si/Al 12.5	50	0[e]	86	14
7	H-Beta Si/Al 12.5	50	75[c]	5	20
8	-	50	4	70	26

[a] 1g of substrate for 90 wt% aqueous LA solution and L_2A or 1.66g for 50 wt% aqueous LA solution was reacted in 10 mL of toluene with 0.5 g of zeolite (except for entry 1 and 8), for 3 h, with the oil bath at 403 K. [b] contains 35% of oligomers inherently. [c] Non-optimal conditions (feedstock, T of oil bath, …). Yields over 80 % are attainable in optimal conditions. [d] L_2A was produced by hydrolysis of 4 g of pure L,L-lactide in 5 g of H_2O with Amberlyst-15 catalyst for 0.5 h at 348 K. This converts about 70 % of the lactide into L_2A. The resulting mixture is still devoid of LA. L_2A could be isolated in 98 % purity from the water phase, in a liquid-liquid extraction of the hydrolysis mixture with toluene for removing remaining lactide. [e] reaction without custom trap for water-removal installed (see Methods and Fig. S1) between reactor and condenser. In this way, water along with toluene refluxes to the reaction and no lactide is formed. Water-removal is essential to the process.

References and Notes

1. K. L. Law, R. C. Thompson, Microplastics in the seas. *Science* **345**, 144–145 (2014). Medline doi:10.1126/science.1254065

2. R. A. Gross, B. Kalra, Biodegradable polymers for the environment. *Science* **297**, 803–807 (2002). Medline doi:10.1126/science.297.5582.803

3. R. Auras, L.-T. Lim, S. E. M. Selke, H. Tsuji, Eds., *Poly(Lactic Acid): Synthesis, Structures, Properties, Processing, and Applications*. (Wiley, New York, 2010).

4. L. Shen, E. Worrell, M. Patel, Present and future development in plastics from biomass. *Biofuels Bioprod. Biorefin.* **4**, 25–40 (2010). doi:10.1002/bbb.189

5. C. O. Tuck, E. Pérez, I. T. Horváth, R. A. Sheldon, M. Poliakoff, Valorization of biomass: Deriving more value from waste. *Science* **337**, 695–699 (2012). Medline doi:10.1126/science.1218930

6. E. T. H. Vink, K. R. Rábago, D. A. Glassner, P. R. Gruber, Applications of life cycle assessment to NatureWorks™ polylactide (PLA) production. *Polym. Degrad. Stabil.* **80**, 403–419 (2003). doi:10.1016/S0141-3910(02)00372-5

7. M. S. Holm, S. Saravanamurugan, E. Taarning, Conversion of sugars to lactic acid derivatives using heterogeneous zeotype catalysts. *Science* **328**, 602–605 (2010). Medline doi:10.1126/science.1183990

8. M. Dusselier, P. Van Wouwe, A. Dewaele, E. Makshina, B. F. Sels, *Energy Environ. Sci.* **6**, 1415 (2013).

9. L. S. Sharninghausen, J. Campos, M. G. Manas, R. H. Crabtree, Efficient selective and atom economic catalytic conversion of glycerol to lactic acid. *Nat. Commun.* **5**, 5084 (2014). Medline doi:10.1038/ncomms6084

10. M. A. Abdel-Rahman, Y. Tashiro, K. Sonomoto, Recent advances in lactic acid production by microbial fermentation processes. *Biotechnol. Adv.* **31**, 877–902 (2013). Medline doi:10.1016/j.biotechadv.2013.04.002

11. M. Mueller, European patent 261572A1 (1988).

12. P. R. Gruber *et al*., U.S. patent 5247058 (1993).

13. W. G. O'Brien, L. A. Cariello, T. F. Wells, WO patent 9606092A1 (1996).

14. D. T. Vu, A. K. Kolah, N. S. Asthana, L. Peereboom, C. T. Lira, D. J. Miller, Oligomer distribution in concentrated lactic acid solutions. *Fluid Phase Equilib.* **236**, 125–135 (2005). doi:10.1016/j.fluid.2005.06.021

15. V. N. Emel'yanenko, S. P. Verevkin, C. Schick, E. N. Stepurko, G. N. Roganov, M. K. Georgieva, The thermodynamic properties of S-lactic acid. *Russ. J. Phys. Chem. A* **84**, 1491–1497 (2010). doi:10.1134/S0036024410090074

16. A. Corma, S. Iborra, A. Velty, Chemical routes for the transformation of biomass into chemicals. *Chem. Rev.* **107**, 2411–2502 (2007). Medline doi:10.1021/cr050989d

17. G. W. Huber, R. D. Cortright, J. A. Dumesic, Renewable alkanes by aqueous-phase reforming of biomass-derived oxygenates. *Angew. Chem. Int. Ed.* **43**, 1549–1551 (2004). doi:10.1002/anie.200353050

18. Y. Román-Leshkov, C. J. Barrett, Z. Y. Liu, J. A. Dumesic, Production of dimethylfuran for liquid fuels from biomass-derived carbohydrates. *Nature* **447**, 982–985 (2007). Medline doi:10.1038/nature05923

19. T. P. Vispute, H. Zhang, A. Sanna, R. Xiao, G. W. Huber, Renewable chemical commodity feedstocks from integrated catalytic processing of pyrolysis oils. *Science* **330**, 1222–1227 (2010). Medline doi:10.1126/science.1194218

20. P. B. Weisz, Molecular shape selective catalysis. *Pure Appl. Chem.* **52**, 2091 (1980). doi:10.1351/pac198052092091

21. A. Corma, Inorganic solid acids and their use in acid-catalyzed hydrocarbon reactions. *Chem. Rev.* **95**, 559–614 (1995). doi:10.1021/cr00035a006

22. P. A. Jacobs, M. Dusselier, B. F. Sels, Will zeolite-based catalysis be as relevant in future biorefineries as in crude oil refineries? *Angew. Chem. Int. Ed.* **53**, 8621–8626 (2014). doi:10.1002/anie.201400922

23. C. W. Jones, K. Tsuji, M. E. Davis, Organic-functionalized molecular sieves as shape-selective catalysts**.** *Nature* **393**, 52–54 (1998). doi:10.1038/29959

24. Y.-T. Cheng, Z. Wang, C. J. Gilbert, W. Fan, G. W. Huber, Production of *p*-xylene from biomass by catalytic fast pyrolysis using ZSM-5 catalysts with reduced pore openings. *Angew. Chem. Int. Ed.* **51**, 11097–11100 (2012). doi:10.1002/anie.201205230

25. G. Ertl, H. Knözinger, F. Schüth, J. Weitkamp, *Handbook of Heterogeneous Catalysis* (Wiley-VCH, Weinheim, Germany, ed. 2, 2008).

26. J.-P. Lange, W. D. van de Graaf, R. J. Haan, Conversion of furfuryl alcohol into ethyl levulinate using solid acid catalysts. *ChemSusChem* **2**, 437–441 (2009). Medline doi:10.1002/cssc.200800216

27. B. Smit, T. L. M. Maesen, Towards a molecular understanding of shape selectivity. *Nature* **451**, 671–678 (2008). Medline doi:10.1038/nature06552

28. M. Dusselier, P. Van Wouwe, S. De Smet, R. De Clercq, L. Verbelen, P. Van Puyvelde, F. E. Du Prez, B. F. Sels, Toward functional polyester building blocks from renewable glycolaldehyde with sn cascade catalysis. *ACS Catal.* **3**, 1786–1800 (2013). doi:10.1021/cs400298n

29. W. W. Gerhardt, D. E. Noga, K. I. Hardcastle, A. J. García, D. M. Collard, M. Weck, Functional lactide monomers: Methodology and polymerization. *Biomacromolecules* **7**, 1735–1742 (2006). Medline doi:10.1021/bm060024j

30. P. P. Pescarmona, K. P. F. Janssen, C. Delaet, C. Stroobants, K. Houthoofd, A. Philippaerts, C. De Jonghe, J. S. Paul, P. A. Jacobs, B. F. Sels, Zeolite-catalysed conversion of C3 sugars to alkyl lactates. *Green Chem.* **12**, 1083 (2010). doi:10.1039/b921284a

31. S. Inkinen, M. Hakkarainen, A.-C. Albertsson, A. Södergård, From lactic acid to poly(lactic acid) (PLA): Characterization and analysis of PLA and its precursors. *Biomacromolecules* **12**, 523–532 (2011). Medline doi:10.1021/bm101302t

32. J. L. Espartero, I. Rashkov, S. M. Li, N. Manolova, M. Vert, NMR Analysis of Low Molecular Weight Poly(lactic acid)s. *Macromolecules* **29**, 3535–3539 (1996). doi:10.1021/ma950529u

33. Q. H. Xia, S. C. Shen, J. Song, S. Kawi, K. Hidajat, Structure, morphology, and catalytic activity of β zeolite synthesized in a fluoride medium for asymmetric hydrogenation. *J. Catal.* **219**, 74–84 (2003). doi:10.1016/S0021-9517(03)00154-4

34. K. W. Kim, S. I. Woo, Synthesis of high-molecular-weight poly(L-lactic acid) by direct polycondensation. *Macromol. Chem. Phys.* **203**, 2245–2250 (2002). doi:10.1002/1521-3935(200211)203:15<2245::AID-MACP2245>3.0.CO;2-3

35. Y. M. Harshe, G. Storti, M. Morbidelli, S. Gelosa, D. Moscatelli, Polycondensation kinetics of lactic acid. *Macromol. React. Eng.* **1**, 611–621 (2007). doi:10.1002/mren.200700019

36. A. L. W. Demuynck, P. Levecque, A. Kidane, D. W. Gammon, E. Sickle, P. A. Jacobs, D. E. De Vos, B. F. Sels, Retro-Diels-Alder reactions of masked cyclopentadienones catalyzed by heterogeneous Brønsted acids. *Adv. Synth. Catal.* **352**, 3419–3430 (2010). doi:10.1002/adsc.201000571

37. IZA-Structure-Commission, *Database of Zeolite Structures*, www.iza-online.org/.

38. P. Degée, P. Dubois, R. Jerome, Bulk polymerization of lactides initiated by aluminium isopropoxide, 2. Beneficial effect of lewis bases and transfer agents. *Macromol. Chem. Phys.* **198**, 1973–1984 (1997). doi:10.1002/macp.1997.021980623

39. O. Dechy-Cabaret, B. Martin-Vaca, D. Bourissou, Controlled ring-opening polymerization of lactide and glycolide. *Chem. Rev.* **104**, 6147–6176 (2004). Medline doi:10.1021/cr040002s

40. T. Holm, Aspects of the mechanism of the flame ionization detector. *J. Chromatogr. A* **842**, 221–227 (1999). doi:10.1016/S0021-9673(98)00706-7

41. M. Yin, G. L. Baker, Preparation and characterization of substituted polylactides. *Macromolecules* **32**, 7711–7718 (1999). doi:10.1021/ma9907183